

High Breakdown Voltage ZnO Varistors Obtained by Pressureless Sintering

P. Q. Mantas & J. L. Baptista

Departamento de Engenharia Cerâmica e do Vidro e Centro de Cerâmica e Vidro (INIC),
Universidade de Aveiro, 3800 Aveiro, Portugal

(Received 16 May 1989; revised version received 10 November 1989; accepted 24 November 1989)

Abstract

A process is described to obtain ZnO varistors through the controlled precipitation and mixing of the powders used. Pressureless sintering of these powders led to samples with homogeneous microstructures, small grain sizes and high values of breakdown voltage when sintering was conducted at temperatures below 950°C. Although the breakdown voltages per unit thickness of the varistors sintered at lower temperatures were an order of magnitude higher than those sintered at higher temperatures, their breakdown voltages per grain boundary were smaller. These results are interpreted in the framework of the double Schottky barrier model.

In diesem Artikel wird ein Herstellungsprozeß für ZnO-Varistoren beschrieben, bei dem präzipitierte Pulver verwendet wurden. Durch druckloses Sintern bei Temperaturen unter 950°C konnten Proben mit einer homogenen Mikrostruktur, kleinen Korngrößen und hohen Durchbruchspannungen hergestellt werden. Obwohl die Durchbruchspannungen pro Einheitsdicke von Varistoren, die bei niedrigen Temperaturen gesintert wurden, um eine Größenordnung höher liegt, als die von Proben, die bei höheren Temperaturen gesintert wurden, ist deren Durchbruchspannung pro Korngrenze geringer. Die Ergebnisse werden im Rahmen des Doppel-Schottkybarrierenmodells interpretiert.

On décrit ici un procédé d'obtention de résistances variables de ZnO par précipitation contrôlée et mélange des poudres. Le frittage naturel de celles-ci conduit à des échantillons présentant des microstructures homogènes à grains fins et des tensions de rupture élevées pour des températures de frittage inférieures à 950°C. Bien que, pour les échantillons frittés à basses températures, les tensions de rupture

par unité d'épaisseur aient été supérieures d'un ordre de grandeur aux valeurs de ceux frittés à des températures plus élevées, leurs tensions de rupture par joint de grain étaient inférieures. Ces résultats ont été interprétés dans le cadre du modèle de la double barrière de Schottky.

Introduction

The great variety of applications of ZnO varistors for protection of electrical circuits makes them of high technological and economic interest. The performance of these multicomponent and multiphase ceramics is very dependent on the ceramic processing parameters, whose relative importance is sometimes difficult to assess owing to the chemical complexity of these materials.

Since it is well known that, besides the ceramic processing steps, the quality of the starting powders is a very important technological parameter, often conditioning the subsequent processing steps, there has been increasing interest in developing powders of controlled quality for varistor production.^{1–4} Sophisticated methods of powder production could produce varistors sintered at lower temperatures, with a better homogeneity of dopant distribution and improved microstructures, conditions for obtaining better electrical properties. However, market considerations, namely for the high tonnage production of components such as the high voltage surge arrestors used in electrical power stations, impose severe restrictions on the methods used to produce the ceramic powders.

In this work we report a simple method for obtaining intimate mixtures of zinc oxide with some of the most common oxide dopants used in ZnO-based varistor production, namely those of Co, Mn

and Bi. In the simplified system we deliberately avoided introducing Sb, a commonly used component of commercial varistors, thereby excluding from the ceramic microstructure the extra pyrochlore or spinel phase. The aim of this phase exclusion was to have a better assessment of the influence of the sintering temperature, densification and ZnO grain size on the electrical properties of the varistors obtained. Some preliminary results obtained by using the method here described were previously reported.⁵

Results and Discussion

Coprecipitation procedure

To produce mixed powders for ZnO varistor compositions containing Co, Mn and Bi, we used a two-step process. In the first step coprecipitation of zinc, cobalt and manganese was accomplished by spraying 500 cm³ of a distilled water solution 2.436M in Zn(NO₃)₂·6H₂O, 0.012M in Co(NO₃)₂·6H₂O and 0.012M in Mn(NO₃)₂·4H₂O over a stirred solution of NaOH maintained at pH 12.7 by continuous addition of a 7.7M solution of NaOH. It has been shown that under these conditions ZnO is the only insoluble form of zinc precipitating from solutions of zinc nitrate or zinc chloride salts.^{6,7} Cobalt and manganese would precipitate as hydroxides,⁸ but they could not be detected here on the X-ray diffractograms of the coprecipitated product.

The precipitated powder was separated by filtration using glass sintered G5 filters, washed four times with distilled water, once with ethyl alcohol and, finally, once with acetone. A yield of 99.8% of that theoretically expected was obtained by this preparation method. However, TGA analysis (10°C min⁻¹) showed a weight loss of 3.3% occurring almost continuously between room temperature and about 800°C, probably due to the loss of physically and chemically adsorbed water. Table 1 shows the chemical and physical characteristics of the prepared powder. Co, Mn and Na were determined by atomic absorption spectroscopy, crystallite size by X-ray line broadening measurements, and specific

Table 1. Characteristics of the coprecipitated powders

Chemical analysis			Physical characteristics	
CoO (mol%)	MnO (mol%)	Na (wt ppm)	Crystallite size (X-ray) (μm)	Surface area (BET) (m ² g ⁻¹)
0.494	0.416	60.8	0.141	8

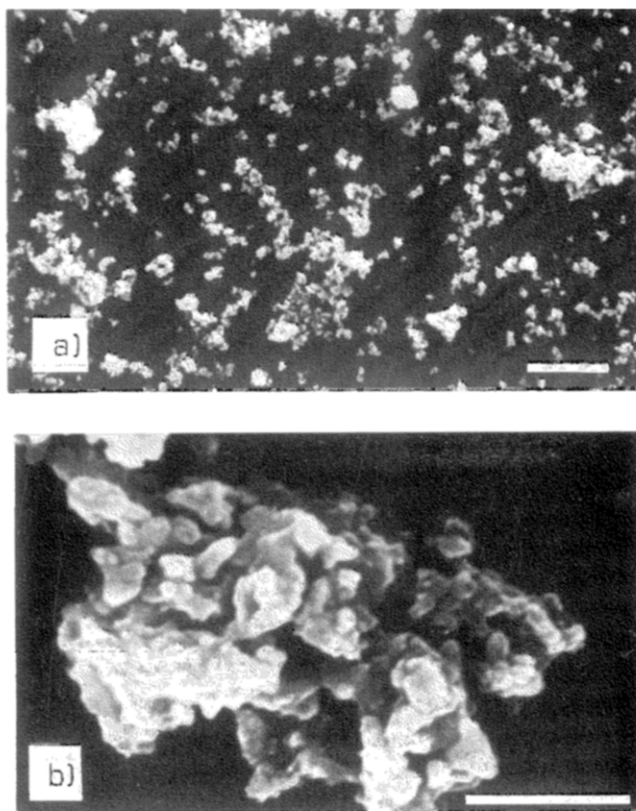


Fig. 1. Photomicrographs of the powder: (a) general aspect of the powder (bar = 10 μm); (b) agglomerate (bar = 1 μm).

surface area by N₂ adsorption. Figure 1 shows photomicrographs of the powder. It can be seen that the powder consists of small particles about 1 μm in size or less, most of them forming agglomerates.

The particle size distribution obtained by LASER light scattering, before and after submitting a suspension of the powder to an ultrasonic treatment during 30 min, is shown in Fig. 2. A narrow frequency distribution is obtained by the ultrasonic

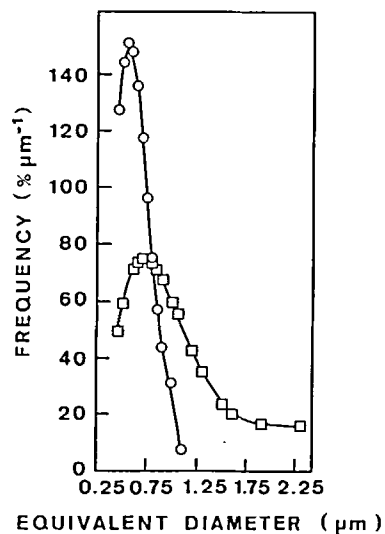


Fig. 2. Particle size distribution of the powder (□) as prepared and (○) after 30 min of ultrasonic treatment. The maximum value for the particle size was 5 and 2 μm, respectively.

breaking of the larger agglomerates. The powder characteristics, namely particle size and shape and the state of agglomeration, can be altered by manipulating several parameters, such as pH, temperature, concentration and rate or order of addition of reagents. The size of the droplets obtained from the spraying nozzle and the presence of dispersants in the medium will also play a role in the characteristics of the precipitated powders. Some of these parameters are under investigation, but the powder characteristics described above were considered sufficient for the present study.

Electrostatic mixing

The second step for producing mixed powders to obtain varistor compositions containing Co, Mn and Bi consisted of mixing Bi_2O_3 powder with the powder produced by the coprecipitation method described. The procedure adopted relied on trying to achieve a homogeneous mixture, by stirring the suspensions where the electrical surface charge of each kind of particle had a different sign. In this way not only could a milling-mixing step be avoided (prone to chemical contamination and time and energy consuming) but also there exists the possibility of electrostatic interaction mixing between small particles of Bi_2O_3 and particles of $\text{ZnO}(\text{cop})$ of different mean sizes, eventually controlling somehow, in this step, the final microstructure of the varistor. Bi_2O_3 and ZnO form an eutectic melting at about 740°C . Therefore a homogeneous distribution of Bi_2O_3 particles in between the ZnO particles could promote liquid phase sintering at low temperature.

The pH value of a freshly prepared suspension of $\text{ZnO}(\text{cop})$ in water was 7.2, increasing slowly to 7.5 on ageing at room temperature during four days. This suspension is well deflocculated, and microelectrophoretic observation of diluted aliquots (0.5 wt% $\text{ZnO}(\text{cop})$) shows that the surface charge of the $\text{ZnO}(\text{cop})$ particles is positive at this pH. A water suspension of Bi_2O_3 shows a higher pH, around 9, and the suspension is less stable, sedimentation of the particles taking place at a higher rate.

The small amount of Bi_2O_3 needed to be added to $\text{ZnO}(\text{cop})$ to obtain a varistor composition (0.5 mol% Bi_2O_3) does not alter significantly the pH of the ZnO suspension, which is maintained around the neutral value. To obtain the surface charge of the Bi_2O_3 particles at pH 7, titration of a 0.5 wt% suspension of Bi_2O_3 in water was done using a 10^{-2}M HCl solution. The charge measurement at pH 7 was not straightforward since the pH value of the Bi_2O_3 suspension changes abruptly from 8.3 to

3.2 by a small addition of the HCl solution and then slowly comes back to a value near the previous one. This 'buffer'-like behaviour depended on the particle size of the Bi_2O_3 particles. It seems, therefore, that some kind of surface reaction was taking place at the surface of the Bi_2O_3 particles. After monitoring the kinetic behaviour of the pH recovery, a microelectrophoretic observation of the Bi_2O_3 suspension in the pH range 7.0 ± 0.5 was done with an aliquot of the suspension removed during the recovery time. In this pH range, the one where the particles will find themselves when added to the $\text{ZnO}(\text{cop})$ suspension, the surface charge is negative, i.e. opposite to the surface charge of the $\text{ZnO}(\text{cop})$ particles.

The suspension obtained by adding the Bi_2O_3 suspension to the $\text{ZnO}(\text{cop})$ suspension continues to be well deflocculated. Some trial runs were done where the bismuth oxide concentration was greatly increased, up to 5 mol%, to allow a better observation of the suspension behaviour. The neutral suspension continued to be very stable and the powders obtained, even by water evaporation, did not show any sign of differential sedimentation. On the other hand, if the mixing was conducted with adjustment of the pH to around 9, differential sedimentation took place with colour bands clearly seen in the sediment.

The absence of differential sedimentation at neutral pH seems to indicate that some sort of interaction took place between the two kinds of particles. Based on the experiments described we therefore suggest that this interaction is of an electrostatic nature.

As a standard procedure, to prepare the 99.5 mol% $\text{ZnO}(\text{cop}) + 0.5$ mol% Bi_2O_3 composition we adopted the following method. The Bi_2O_3 suspension was added to the $\text{ZnO}(\text{cop})$ suspension at neutral pH while stirring. The mixed powder suspension was quickly filtered, with suction, over a glass sintered G5 filter. Absolute ethanol and acetone were passed through the filter, without disturbing the settled powder. After drying at 110°C the powder obtained was used in the sintering experiments.

Before sintering no previous calcination of the powders was done. The weight loss determined by TGA, using the same heating rate as used in sintering experiments was only 0.2 wt% between 700 and 800°C , the region where the appearance of the eutectic liquid could promote sintering.

Sintering and electrical characteristics

Samples of the coprecipitated powders and of these powders mixed with Bi_2O_3 were pressed into discs

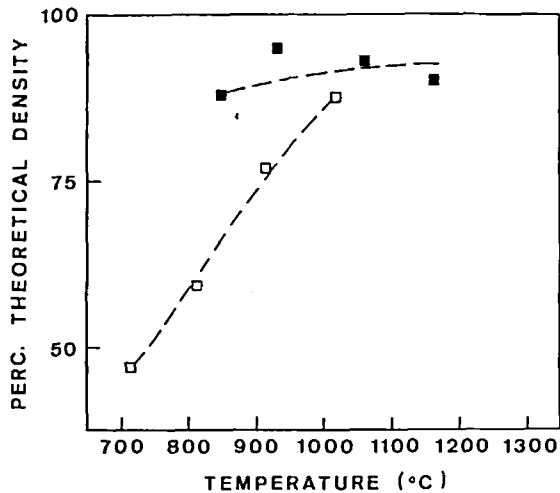


Fig. 3. Densities with (■) and without (□) Bi_2O_3 addition as a function of sintering temperature. The sintering time was 2 h.

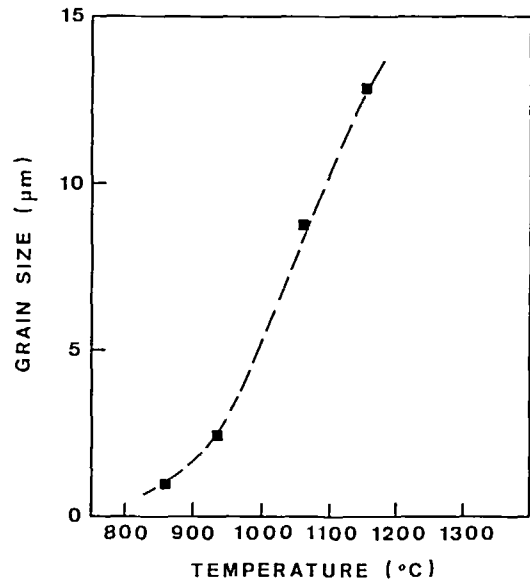


Fig. 5. Mean grain size as a function of sintering temperature. The sintering time was 2 h.

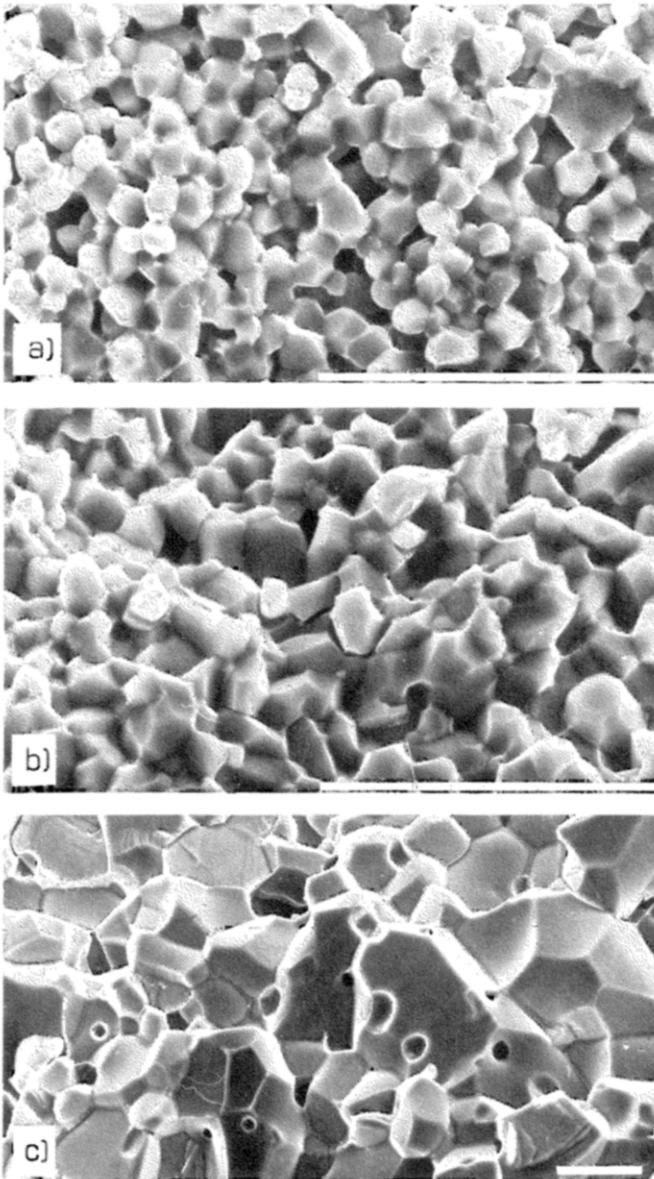


Fig. 4. Photomicrographs of fractured surfaces obtained by SEM: (a) sample sintered at 857°C; (b) at 934°C; and (c) at 1153°C (bar = 10 μm). The sintering time was 2 h.

2 cm in diameter and 1 to 2 mm thick and sintered in air at different temperatures for 2 h. Heating rates to sintering temperatures were $10^\circ\text{C min}^{-1}$. Figure 3 presents the densities observed for samples sintered before and after the addition of Bi_2O_3 . Although a complete sintering study was not undertaken, it is clear that the addition of Bi_2O_3 promotes densification at lower temperatures, which would be expected from the presence of the eutectic liquid. For the Bi_2O_3 -containing samples, the density variations observed in the range of temperatures tried is small, but the highest density (96% of theoretical density) is achieved at the 934°C isothermal sintering. SEM micrographs of fractured surfaces of the Bi_2O_3 -containing samples sintered at different temperatures are presented in Fig. 4. All the samples show reasonably uniform microstructures and the mean grain sizes determined from them are presented in Fig. 5. Grain sizes remain small for samples sintered at the lowest temperatures. Grain coarsening seems to start around 1000°C, the grain size being already about 10 μm for samples sintered at 1060°C. The lower densities attained at temperatures above 934°C are probably the result of the grain growth occurring concomitant with densification in these samples. Loss of Bi_2O_3 by evaporation could also be thought as responsible for lower densities attained, but this loss has been reported to occur for much higher sintering temperatures than these.⁹

Measurements of the current/voltage characteristics of samples containing Bi_2O_3 were done as described previously (see, e.g., Ref. 10). Figure 6 presents the I-V characteristics of the varistors obtained. As a general trend it is seen that samples

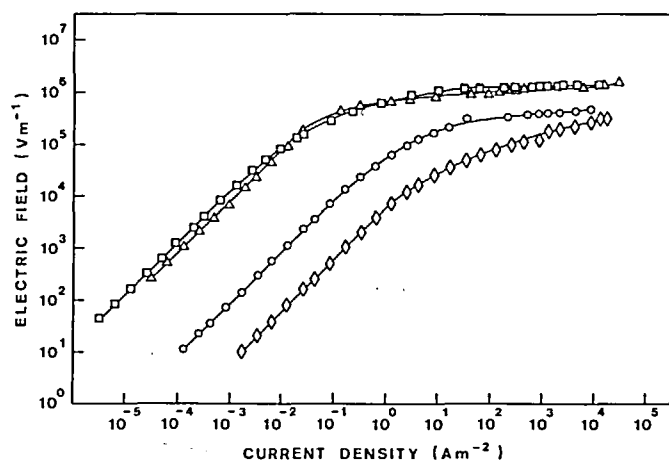


Fig. 6. I-V curves, taking the geometry of the samples, for samples sintered at: (Δ) 857°C; (\square) 934°C; (\circ) 1060°C; and (\diamond) 1153°C.

sintered at lower temperatures tend to have high resistivities in the ohmic region and high values of breakdown voltage, both decreasing steadily with the increase in sintering temperature. The same effect, namely the decrease in resistivity, was described for samples prepared by a urea method and hot pressed between 750 and 900°C.² Higher breakdown voltages were also previously reported for hot-pressed samples obtained from sol-gel processed powders.¹ In both cases the hot-pressed samples had to go through a reoxidation procedure to develop the varistor characteristics, which was perhaps the origin of the great variability of the electrical properties observed between similar samples and between different parts of the same sample. Recently, pressureless sintering of varistor samples with high breakdown voltages was achieved by sintering above 1050°C powders prepared by an amine precipitation method.⁴

It is interesting to note that the densities and the mean grain sizes obtained in this work, for samples pressureless sintered in the same temperature range as the hot-pressed samples of the previous works,^{1,2} have similar values, and that, although the com-

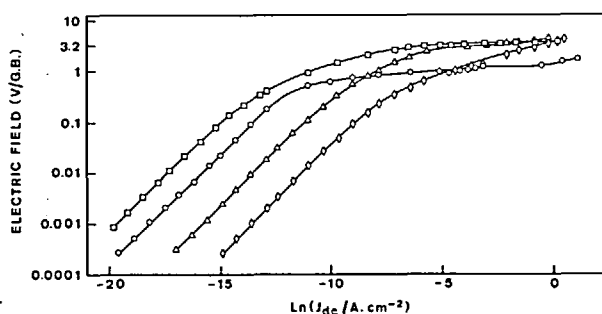


Fig. 7. I-V curves, taking the mean grain size of the samples, for samples sintered at: (\circ) 857°C; (\square) 934°C; (Δ) 1060°C; and (\diamond) 1153°C.

Table 2. Variation of ohmic resistivity and breakdown voltage with sintering temperature

Sintering temperature (°C)	Ohmic resistivity (Ωm)	Breakdown voltage per thickness (Vmm^{-1}) ^a	Breakdown voltage per grain boundary (V/GB)
857	6.31×10^6	764	1.3
934	1.29×10^7	794	3.2
1060	7.94×10^4	191	3.2
1153	6.31×10^3	26	3.1

^aAt 1 mA cm⁻².

position used here is a simpler one, similar electrical effects were observed, as already reported.⁵

Although the high breakdown voltages observed in Fig. 6 for samples sintered at lower temperatures and having small grain sizes were somewhat expected due to the higher number of barrier heights existing between the electrodes, each one associated with the ZnO-ZnO grain boundary, it was unlikely that this simple explanation could account for the observed variations in the I-V curves. In Fig. 7 we have redrawn the I-V curves taking into account the thickness of the sample and the mean grain size for the different sintering temperatures, obtaining therefore the variation of the voltage per grain boundary as a function of the current density. The uniformity of the microstructures justifies this procedure.

Two features can be observed in Fig. 7: the resistivity in the ohmic region increases for samples sintered up to 934°C and then decreases; and the breakdown voltage per grain boundary, V_b ,[†] increases up to 934°C and then stabilizes at a value around 3.2 V. These values are presented in Table 2 together with values for the breakdown voltage per unit thickness. Figure 8 shows, for the same samples, values for the barrier height, E_b , determined using the Blatter and Greuter model,^{11,12} the concentration of ionized donors, N_d , determined from C-V measurements at the frequency of 1 MHz,¹⁰ and the values for the concentration of surface states, N_t , calculated from E_b and N_d .¹⁰ The values of N_d and N_t show little variation until the sintering temperature of 1060°C is reached and then decrease sharply. The barrier height, E_b , has a maximum value for the sample sintered at 934°C, where the voltage per

[†]In commercial varistors V_b is usually taken as the voltage at 1 mA cm⁻² of current density, where normally a flat region, parallel to the current axis, sets up. To allow testing current varistor models, we considered here that a much better value for this parameter would be near the region of 'upturn', before the conduction started to be controlled by the bulk ZnO grain resistivity.

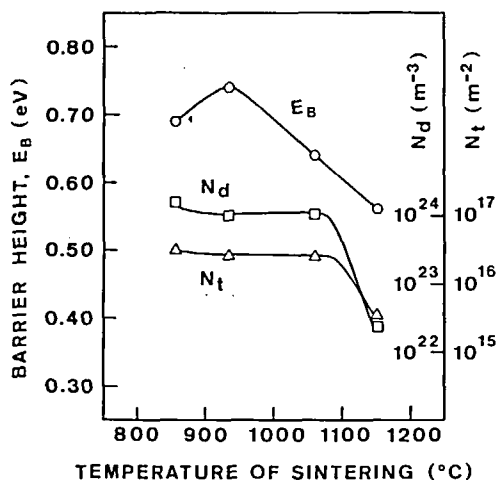


Fig. 8. Values of (○) barrier height, E_b , (□) concentration of ionized donors, N_d , and (△) concentration of surface states, N_t , as a function of sintering temperature.

grain boundary attained also its maximum value, but, apart from that, it seems that E_b and V_b are not correlated in a straightforward manner.

A breakdown voltage of ~ 3.2 V per grain boundary, a value commonly observed for varistor samples sintered at temperatures around 1300°C , is usually related to the band gap of ZnO ($E_g \sim 3.2$ eV at room temperature).^{11,13-15} Since this will correspond to the energy difference of the Fermi levels between two adjacent ZnO grains at high electric fields, it has been argued that electrons can then be ionized directly from the valence band of one ZnO grain to the conduction band of the adjacent one, since these states would be a short distance apart across the junction (~ 50 nm).^{14,16} As an alternative, it has been proposed¹³⁻¹⁵ that when $eV + E_b > E_g$, V being the applied voltage, some electrons that cross the junction will have enough kinetic energy to impact-ionize electrons from the valence band, generating electron-hole pairs, whose recombination has been detected.^{13,14}

The models just presented cannot explain values of V_b lower than 3.2 V, like the ones observed for samples sintered below 934°C in this work and reported in other works.^{17,18} In fact it is only consistent with very high local fields (1 MV cm^{-1}) being built up near the interface.¹⁹ The local field there developing will depend on the space charge distribution near the grain boundary. In real systems it will depend on the width of the depletion layers and on the resistivity of the bulk ZnO grains. If the resistivity of the ZnO grains is high enough, in a way that there is a substantial drop of the electric field through the grain, it is expected that the local field near the grain boundary will be smaller than when the grains have low resistivity. The same applies to

very large depletion layers. In other words, to achieve a value of $V_b \sim 3.2$ V, it is necessary to have conductive grains and a very large potential energy perturbation localized near the grain boundaries.

The breakdown regime can be regarded as a consequence of the vanishing of the barrier height. This regime will be achieved when all the surface states in the interface are occupied.^{11,20} This can happen, for samples with high resistivity grains or large depletion layers, before high local fields can be developed in the grain boundary region, and smaller values than 3.2 V are therefore expected for the breakdown voltage. This is probably what happens in samples sintered at lower temperatures when the segregation of bismuth to the interface during cooling down would perhaps be less marked than when the cooling took place from samples sintered at higher temperatures.²¹ Also the increase in the sintering temperature leads to an increase in the intrinsic and/or extrinsic concentration of donors in the bulk of ZnO grains, increasing therefore the bulk conductivity. Both phenomena will lead to high fields developing at the grain boundary for samples sintered at higher temperatures, allowing the value of 3.2 V being attained for V_b .

The increase in leakage currents occurring for the samples sintered at higher temperatures is also probably related to an increase in the concentration of extrinsic donors. This effect has been observed for varistor samples doped with Mn¹⁶ and accounted for by the production of deep traps,^{11,12} because they control somehow the barrier height. The significant decrease in N_d and N_t occurring for samples sintered at higher temperatures also agrees with a faster filling up of the interfaces states, promoting a quick decay of the barrier height.

Conclusion

Zinc oxide was doped with cobalt and manganese by using a coprecipitation method that can be extended to many other of the common dopants used in varistor production. A mixing procedure was developed to promote homogeneous mixing of the coprecipitated powder with Bi_2O_3 , less prone to contamination than the usual milling-mixing step. Sintering of the varistor compositions could be conducted at lower temperatures (~ 850 – 950°C) where grain growth is incipient. Densifications up to 96% of theoretical density could be achieved by pressureless sintering at temperatures below 1000°C , maintaining uniform microstructures and small

grain sizes. The breakdown voltages of the resulting varistors were therefore considerably increased, although the breakdown voltage per grain boundary was smaller than that of samples sintered at higher temperatures.

References

1. Lauf, R. J. & Bond, W. D., Fabrication of high-field zinc oxide varistors by sol-gel processing. *Am. Ceram. Soc. Bull.*, **63**(2) (1984) 278.
2. Sonder, H., Quimby, T. C. & Kinser, D. L., ZnO varistors made from powders produced using a urea process. *Am. Ceram. Soc. Bull.*, **65**(4) (1986) 665.
3. Ivers-Tiffée, E. & Seitz, K., Characterization of varistor-type raw materials prepared by the evaporative decomposition of solutions technique. *Am. Ceram. Soc. Bull.*, **66**(9) (1987) 1384.
4. Hishita, S., Yao, Y. & Shirasaki, S., Zinc oxide varistors made from powders prepared by amine processing. *J. Am. Ceram. Soc.*, **72**(2) (1989) C338.
5. Simões, J. A. R., Mantas, P. Q. & Baptista, J. L., Electrical properties of doped ZnO ceramics obtained by controlled chemical synthesis of powders. Presented at *Electroceramics II, International Conference*, Brussels, 21–23 September 1988. To be published in the Conference Proceedings.
6. Takada, T., Kiyama, M., Torii, H., Asai, T., Takano, M. & Nakanishi, N., Effect of pH values on the formation and solubility of zinc compounds. *Bull. Inst. Chem. Res., Kyoto Univ.*, **56** (1978) 242.
7. Costa, M. E. V., Diz, H. M. M. & Baptista, J. L., The influence of deflocculants on the precipitation, conformation and sintering behaviour of zinc oxide powders. In *Science of Ceramics 14*, ed. Derek Taylor. The Institute of Ceramics, Stoke-on-Trent, UK, 1988, p. 299.
8. Weast, R. C. & Astle, M. J. (eds), *Handbook of Chemistry and Physics*, 61st edn. CRC Press, Boca Raton, FL, 1980–81.
9. Wong, J., Sintering and varistor characteristics of ZnO–Bi₂O₃ ceramics. *J. Appl. Phys.*, **51**(8) (1980) 4453.
10. Senos, A. M. R. & Baptista, J. L., Atmosphere effects in the grain boundary region of ZnO varistors. *J. Mater. Sci. Lett.*, **3** (1984) 213.
11. Blatter, G. & Greuter, F., Carrier transport through grain boundaries in semiconductors. *Phys. Rev.*, **B33**, **6** (1986) 3952.
12. Greuter, F., Blatter, G., Rossinelli, M. & Schmücle, F., Bulk and grain boundary defects in polycrystalline ZnO. In *Defects in Semiconductors*, ed. H. J. von Bardeleben. *Mater. Sci. Forum*, **10–12** (1986) 235.
13. Rossinelli, M., Blatter, G. & Greuter, F., Grain boundary properties of ZnO varistors. In *Electrical Ceramics*, ed. B. C. H. Steele. *Br. Ceram. Proc.*, **36**(1) (1985) 1.
14. Mahan, G. D., Theory of ZnO varistors, *Mater. Res. Soc. Symp. Proc.*, Vol. 5, ed. H. J. Leamy, G. E. Pike & C. H. Seager. North-Holland, Amsterdam, 1982, p. 333.
15. Pike, G. E., Electronic properties of ZnO varistors: a new model. *Ibid.*, p. 369.
16. Schwing, U. & Hoffmann, B., Model experiments describing the microcontact of ZnO varistors. *J. Appl. Phys.*, **57**(12) (1985) 5372.
17. Suyama, Y., Microstructure and property of ZnO varistors fabricated from fine powders. In *High Tech Ceramics*, Mater. Sci. Monographs, Vol. 38B, ed. P. Vincenzini. Elsevier, Amsterdam, 1987, p. 1775.
18. Sletson, L. C., Potter, M. E. & Alim, M. A., Influence of sintering temperature on intrinsic trapping in zinc oxide-based varistors. *J. Am. Ceram. Soc.*, **71**(11) (1988) 909.
19. Blatter, G. & Greuter, F., Electrical breakdown at semiconductor grain boundaries. *Phys. Rev.*, **B34**, **12** (1986) 8555.
20. Pike, G. E. & Seager, C. H., The dc voltage dependence of semiconductor grain-boundary resistance. *J. Appl. Phys.*, **50** (1979) 3414.
21. Mantas, P. Q. & Baptista, J. L., Grain boundary phenomena in ZnO varistors. In *High Tech Ceramics*, Mater. Sci. Monographs, Vol. 38B, ed. P. Vincenzini. Elsevier, Amsterdam, 1987, p. 1791.